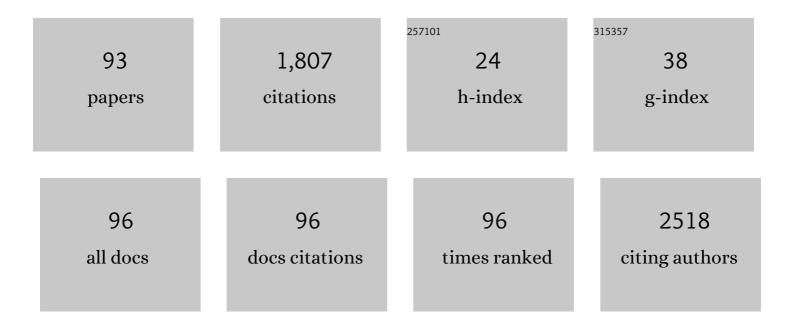
David Horwat

List of Publications by Year in descending order

Source: https://exaly.com/author-pdf/1407888/publications.pdf Version: 2024-02-01



ΠΑΝΙΟ ΗΟΡΜΑΤ

#	Article	IF	CITATIONS
1	Rapid ellipsometric determination and mapping of alloy stoichiometry with a neural network. Optics Letters, 2022, 47, 2117.	1.7	2
2	Composition-driven transition from amorphous to crystalline films enables bottom-up design of functional surfaces. Applied Surface Science, 2021, 538, 148133.	3.1	8
3	Influence of magnesium doping on microstructure, optical and photocatalytic activity of zinc oxide thin films synthesis by sol–gel route. Applied Physics A: Materials Science and Processing, 2021, 127, 1.	1.1	11
4	Growth kinetics and origin of residual stress of two-phase crystalline–amorphous nanostructured films. Journal of Applied Physics, 2021, 129, .	1.1	5
5	Elaboration of high-transparency ZnO thin films by ultrasonic spray pyrolysis with fast growth rate. Superlattices and Microstructures, 2021, 156, 106945.	1.4	7
6	White light emission from Sm-doped YAG ceramic controlled by the excitation wavelengths. Optics and Laser Technology, 2021, 142, 107223.	2.2	4
7	Ag-based electrocatalysts for ethylene epoxidation. Electrochimica Acta, 2021, 394, 139018.	2.6	4
8	Blue emission and twin structure of p-type copper iodide thin films. Surfaces and Interfaces, 2021, 27, 101500.	1.5	6
9	Towards enhanced durability of electrochromic WO3 interfaced with liquid or ceramic sodium-based electrolytes. Electrochimica Acta, 2020, 360, 136931.	2.6	20
10	Morphological and chemical dynamics upon electrochemical cyclic sodiation of electrochromic tungsten oxide coatings extracted by in situ ellipsometry. Applied Optics, 2020, 59, 3766.	0.9	6
11	Controlling surface morphology by nanocrystalline/amorphous competitive self-phase separation in thin films: Thickness-modulated reflectance and interference phenomena. Acta Materialia, 2019, 181, 78-86.	3.8	11
12	Semi-Transparent p-Cu ₂ O/n-ZnO Nanoscale-Film Heterojunctions for Photodetection and Photovoltaic Applications. ACS Applied Nano Materials, 2019, 2, 4358-4366.	2.4	49
13	Ultraviolet to infrared downshifting in Ce and Yb co-doped aluminum oxynitride thin films. Journal Physics D: Applied Physics, 2019, 52, 285105.	1.3	Ο
14	Growth, interfacial microstructure and optical properties of NiO thin films with various types of texture. Acta Materialia, 2019, 164, 648-653.	3.8	24
15	Coloration mechanism of electrochromic Na _x WO ₃ thin films. Optics Letters, 2019, 44, 1104.	1.7	13
16	Enhancing oxygen reduction reaction of YSZ/La2NiO4+δ using an ultrathin La2NiO4+δ interfacial layer. Journal of Alloys and Compounds, 2018, 746, 413-420.	2.8	25
17	Electrochemical promotion of propylene combustion on Ag catalytic coatings. Catalysis Communications, 2018, 104, 28-31.	1.6	6
18	Wurtzite CoO: a direct band gap oxide suitable for a photovoltaic absorber. Chemical Communications, 2018, 54, 13949-13952.	2.2	21

#	Article	IF	CITATIONS
19	Tunable Localized Surface Plasmon Resonance and Broadband Visible Photoresponse of Cu Nanoparticles/ZnO Surfaces. ACS Applied Materials & Interfaces, 2018, 10, 40958-40965.	4.0	26
20	Local Structure and Point-Defect-Dependent Area-Selective Atomic Layer Deposition Approach for Facile Synthesis of p-Cu ₂ 0/n-ZnO Segmented Nanojunctions. ACS Applied Materials & Interfaces, 2018, 10, 37671-37678.	4.0	17
21	WTe ₂ Synthesis by Tellurization of W Precursors Using Isothermal Close Space Vapor Transport Annealing. Physica Status Solidi (A) Applications and Materials Science, 2018, 215, 1800425.	0.8	3
22	From Blue to White Luminescence in Cerium-Doped Aluminum Oxynitride: Electronic Structure and Local Chemistry Perspectives. Journal of Physical Chemistry C, 2018, 122, 21623-21631.	1.5	6
23	Local Homoepitaxial Growth in Sputtered NiO Thin Films: An Effective Approach to Tune the Crystallization, Preferred Growth Orientation, and Electrical Properties. Physica Status Solidi - Rapid Research Letters, 2018, 12, 1800191.	1.2	2
24	Ultraviolet optical excitation of near infrared emission of Yb-doped crystalline aluminum oxynitride thin films. Journal of Applied Physics, 2018, 124, 033102.	1.1	2
25	Effect of substrate temperature on the deposition of Al-doped ZnO thin films using high power impulse magnetron sputtering. Surface and Coatings Technology, 2018, 347, 245-251.	2.2	25
26	Restoring the Properties of Transparent Al-Doped ZnO Thin Film Electrodes Exposed to Ambient Air. Journal of Physical Chemistry C, 2017, 121, 14426-14433.	1.5	10
27	Nitrogen chemical state in N-doped Cu2O thin films. Applied Physics Letters, 2017, 110, .	1.5	18
28	Room temperature self-assembled growth of vertically aligned columnar copper oxide nanocomposite thin films on unmatched substrates. Scientific Reports, 2017, 7, 11122.	1.6	7
29	Structural and mechanical properties of Zr1â^'x Mox thin films: From the nano-crystalline to the amorphous state. Journal of Alloys and Compounds, 2017, 729, 137-143.	2.8	5
30	Controlling refractive index in AlN films by texture and crystallinity manipulation. Thin Solid Films, 2017, 636, 537-545.	0.8	20
31	Strong Room Temperature Blue Emission from Rapid Thermal Annealed Cerium-Doped Aluminum (Oxy)Nitride Thin Films, ACS Photonics, 2017, 4, 1945-1953. Electronic structures of Amml:math	3.2	12
32	xmlns:mml="http://www.w3.org/1998/Math/MathML"> <mml:mrow> <mml:mi mathvariant="normal">C <mml:msub> <mml:mi mathvariant="normal">u <mml:mn>2</mml:mn> </mml:mi </mml:msub> <mml:mi mathvariant="normal">O <mml:mo>,</mml:mo> <mml:mi< td=""><td>1.1</td><td>202</td></mml:mi<></mml:mi </mml:mi </mml:mrow>	1.1	202
33	mathvariant="normal">C <mml:msub><mml:mi mathvariant="normal" >u<mml:mn>4 Local Structure-Driven Localized Surface Plasmon Absorption and Enhanced Photoluminescence in ZnO-Au Thin Films. Journal of Physical Chemistry C, 2016, 120, 29405-29413.</mml:mn></mml:mi </mml:msub>	1.5	34
34	New strategies for the synthesis of ZnO and Al-doped ZnO films by reactive magnetron sputtering at room temperature. Physica Status Solidi C: Current Topics in Solid State Physics, 2016, 13, 951-957.	0.8	15
35	Room temperature deposition of homogeneous, highly transparent and conductive Al-doped ZnO films by reactive high power impulse magnetron sputtering. Solar Energy Materials and Solar Cells, 2016, 157, 742-749.	3.0	74
36	A novel sputtered Pd mesh architecture as an advanced electrocatalyst for highly efficient hydrogen production. Journal of Power Sources, 2016, 321, 248-256.	4.0	28

#	Article	IF	CITATIONS
37	Bacterial adhesion on biomedical surfaces covered by yttria stabilized zirconia. Journal of Materials Science: Materials in Medicine, 2016, 27, 6.	1.7	11
38	Local heteroepitaxial growth to promote the selective growth orientation, crystallization and interband transition of sputtered NiO thin films. CrystEngComm, 2016, 18, 1732-1739.	1.3	8
39	Tuning the structure and preferred orientation in reactively sputtered copper oxide thin films. Applied Surface Science, 2015, 335, 85-91.	3.1	44
40	Transmittance enhancement and optical band gap widening of Cu2O thin films after air annealing. Journal of Applied Physics, 2014, 115, .	1.1	85
41	Probing temperature-induced ordering in supersaturated Ti1â^'xAlxN coatings by electronic structure. Surface and Coatings Technology, 2014, 242, 207-213.	2.2	2
42	Comparative analysis of Cr-B coatings deposited by magnetron sputtering in DC and HIPIMS modes. Technical Physics Letters, 2014, 40, 614-617.	0.2	11
43	Local Modification of the Microstructure and Electrical Properties of Multifunctional Au–YSZ Nanocomposite Thin Films by Laser Interference Patterning. ACS Applied Materials & Interfaces, 2014, 6, 13707-13715.	4.0	5
44	Electrochemical activation of Au nanoparticles for the selective partial oxidation of methanol. Journal of Catalysis, 2014, 317, 293-302.	3.1	13
45	Generalized Effective Medium Theory to Extract the Optical Properties of Two-Dimensional Nonspherical Metallic Nanoparticle Layers. Journal of Physical Chemistry C, 2014, 118, 4899-4905.	1.5	31
46	Mechanisms of Oxidation of NdNiO _{3â^î^} Thermochromic Thin Films Synthesized by a Two-Step Method in Soft Conditions. Journal of Physical Chemistry C, 2014, 118, 5908-5917.	1.5	15
47	Controlling the preferred orientation in sputter-deposited Cu2O thin films: Influence of the initial growth stage and homoepitaxial growth mechanism. Acta Materialia, 2014, 76, 207-212.	3.8	30
48	Influence of solvent on humidity sensing of sol-gel deposited ZnO thin films. EPJ Applied Physics, 2014, 65, 20302.	0.3	4
49	Near-room temperature single-domain epitaxy of reactively sputtered ZnO films. Journal Physics D: Applied Physics, 2013, 46, 235107.	1.3	28
50	Exciton and core-level electron confinement effects in transparent ZnO thin films. Scientific Reports, 2013, 3, .	1.6	109
51	Influence of laser interference patterning on microstructure and friction behavior of gold/yttria-stabilized zirconia nanocomposite thin films. Journal of Materials Research, 2012, 27, 879-885.	1.2	2
52	Thermal decomposition and fractal properties of sputter-deposited platinum oxide thin films. Journal of Materials Research, 2012, 27, 829-836.	1.2	13
53	Efficient, Low Cost Synthesis of Sodium Platinum Bronze Na _{<i>x</i>} Pt ₃ O ₄ . Chemistry of Materials, 2012, 24, 2429-2432.	3.2	6
54	Bacterial adhesion on biomedical surfaces covered by micrometric silver Islands. Journal of Biomedical Materials Research - Part A, 2012, 100A, 1521-1528.	2.1	10

#	Article	IF	CITATIONS
55	High hardness, low Young's modulus and low friction of nanocrystalline ZrW2 Laves phase and Zr1â^'xWx thin films. Journal of Physics and Chemistry of Solids, 2012, 73, 554-558.	1.9	14
56	6th EEIGM International Conference on Advanced Materials Research. IOP Conference Series: Materials Science and Engineering, 2012, 31, 011001.	0.3	1
57	Chemistry, phase formation, and catalytic activity of thin palladium-containing oxide films synthesized by plasma-assisted physical vapor deposition. Surface and Coatings Technology, 2011, 205, S171-S177.	2.2	33
58	Spectral evidence of spinodal decomposition, phase transformation and molecular nitrogen formation in supersaturated TiAlN films upon annealing. Acta Materialia, 2011, 59, 6287-6296.	3.8	35
59	Nano-scale and surface precipitation of metallic particles in laser interference patterned noble metal-based thin films. Applied Surface Science, 2011, 257, 5223-5229.	3.1	12
60	Influence of the nanoscale structural features on the properties and electronic structure of Al-doped ZnO thin films: An X-ray absorption study. Solar Energy Materials and Solar Cells, 2011, 95, 2341-2346.	3.0	35
61	Microstructure of sputter-deposited noble metal-incorporated oxide thin films patterned by means of laser interference. Materials Research Society Symposia Proceedings, 2011, 1339, 1.	0.1	0
62	Antibacterial properties of biomedical surfaces containing micrometric silver islands. Journal of Physics: Conference Series, 2010, 252, 012015.	0.3	2
63	Beneficial silver: antibacterial nanocomposite Ag-DLC coating to reduce osteolysis of orthopaedic implants. Journal of Physics: Conference Series, 2010, 252, 012005.	0.3	6
64	Ion acceleration and cooling in gasless self-sputtering. Applied Physics Letters, 2010, 97, .	1.5	21
65	On the deactivation of the dopant and electronic structure in reactively sputtered transparent Al-doped ZnO thin films. Journal Physics D: Applied Physics, 2010, 43, 132003.	1.3	34
66	Compression and strong rarefaction in high power impulse magnetron sputtering discharges. Journal of Applied Physics, 2010, 108, .	1.1	73
67	Extended X-ray absorption fine structure (EXAFS) investigations of Ti bonding environment in sputter-deposited nanocomposite TiBC/a-C thin films. IOP Conference Series: Materials Science and Engineering, 2010, 12, 012012.	0.3	4
68	Impact of the particles impingement on the electronic conductivity of Al doped ZnO films grown by reactive magnetron sputtering. IOP Conference Series: Materials Science and Engineering, 2010, 12, 012006.	0.3	0
69	Evolution of structural and physical properties upon annealing of sputter-deposited Zr0.84Y0.16-O2films incorporating copper and palladium nanoparticles. IOP Conference Series: Materials Science and Engineering, 2009, 5, 012022.	0.3	0
70	Estimation of thickness of hydrothermal degraded layer in 3Y-TZP by X-ray diffraction. IOP Conference Series: Materials Science and Engineering, 2009, 5, 012023.	0.3	1
71	Thermochromic effect in NdNiO3â^δthin films annealed in ambient air. Journal Physics D: Applied Physics, 2009, 42, 182006.	1.3	15
72	Electronic structure and conductivity of nanocomposite metal (Au, Ag, Cu, Mo)-containing amorphous carbon films. Solid State Sciences, 2009, 11, 1742-1746.	1.5	32

#	Article	IF	CITATIONS
73	Strontium-doped lanthanum manganite coatings crystallised after air annealing of amorphous co-sputtered films. Materials Chemistry and Physics, 2009, 116, 219-222.	2.0	7
74	Oxidation of magnetron sputtered La-Si thin films for solide oxide fuel cell electronlytes. Thin Solid Films, 2009, 517, 1895-1898.	0.8	9
75	Structure Control in Reactively Sputtered Ag/Cu/(Mn)/O Films. Plasma Processes and Polymers, 2009, 6, 393-400.	1.6	8
76	Impact of Annealing on the Conductivity of Amorphous Carbon Films Incorporating Copper and Gold Nanoparticles Deposited by Pulsed Dual Cathodic Arc. Plasma Processes and Polymers, 2009, 6, S438.	1.6	9
77	Silver islands formed after air annealing of amorphous Ag–Cu–Mn–O sputtered films. Journal of Crystal Growth, 2009, 311, 349-354.	0.7	9
78	Effect of annealing temperature on the decomposition of reactively sputtered Ag2Cu2O3 films. Applied Surface Science, 2009, 255, 7700-7702.	3.1	12
79	Structure–properties relationship in reactively sputtered Ag–Cu–O films. Journal Physics D: Applied Physics, 2009, 42, 025304.	1.3	15
80	Properties of nanocrystalline and nanocomposite WxZr1â^'x thin films deposited by co-sputtering. Intermetallics, 2009, 17, 421-426.	1.8	18
81	Deep oxidation of methane on particles derived from YSZ-supported Pd–Pt-(O) coatings synthesized by Pulsed Filtered Cathodic Arc. Catalysis Communications, 2009, 10, 1410-1413.	1.6	9
82	5th International EEIGM/AMASE/FORGEMAT Conference on Advanced Materials Research. IOP Conference Series: Materials Science and Engineering, 2009, 5, 011001.	0.3	2
83	Comparison Between Ultrathin Films of YSZ Deposited at the Solid Oxide Fuel Cell Cathode/Electrolyte Interface by Atomic Layer Deposition, Dip-Coating or Sputtering. Open Fuels and Energy Science Journal, 2009, 2, 87-99.	0.2	0
84	Effect of the oxygen flow rate on the structure and the properties of Ag–Cu–O sputtered films deposited using a Ag/Cu target with eutectic composition. Applied Surface Science, 2008, 254, 6590-6594.	3.1	26
85	Structural-electrical-optical properties relationship of sodium superionic conductor sputter-deposited coatings. Thin Solid Films, 2008, 516, 3387-3393.	0.8	4
86	Towards a thin films electrochromic device using NASICON electrolyte. Ionics, 2008, 14, 227-233.	1.2	8
87	Addition of silver in copper nitride films deposited by reactive magnetron sputtering. Scripta Materialia, 2008, 58, 568-570.	2.6	50
88	Spatial distribution of average charge state and deposition rate in high power impulse magnetron sputtering of copper. Journal Physics D: Applied Physics, 2008, 41, 135210.	1.3	42
89	Magnetron sputtering of NASICON (Na3Zr2Si2PO12) thin films Part I: Limitations of the classical methods. Surface and Coatings Technology, 2007, 201, 7013-7017.	2.2	5
90	Magnetron sputtering of NASICON (Na3Zr2Si2PO12) thin films. Surface and Coatings Technology, 2007, 201, 7060-7065.	2.2	16

#	Article	IF	CITATIONS
91	Influence of the current applied to the silver target on the structure and the properties of Ag–Cu–O films deposited by reactive cosputtering. Applied Surface Science, 2007, 253, 7522-7526.	3.1	30
92	Effects of substrate position and oxygen gas flow rate on the properties of ZnO: Al films prepared by reactive co-sputtering. Thin Solid Films, 2007, 515, 5444-5448.	0.8	48
93	Sodium superionic conductor sputter-deposited coatings. Ionics, 2005, 11, 120-125.	1.2	7